

Fatty acid amide hydrolase inhibitors display broad selectivity and inhibit multiple carboxylesterases as off-targets

Di Zhang*, Anita Saraf¹, Teodozyi Kolasa, Pramila Bhatia, Guo Zhu Zheng, Meena Patel, Greg S. Lannoye, Paul Richardson, Andrew Stewart, John C. Rogers, Jorge D. Brioni, Carol S. Surowy

Neuroscience Research, Advanced Technology and Process Research and Development, Global Pharmaceutical Research and Development, Abbott Laboratories, Abbott Park, IL 60064, USA

Received 4 October 2006; received in revised form 22 November 2006; accepted 27 November 2006

Abstract

Fatty acid amide hydrolase (FAAH) is the primary regulator of several bioactive lipid amides including anandamide. Inhibitors of FAAH are potentially useful for the treatment of pain, anxiety, depression, and other nervous system disorders. However, FAAH inhibitors must display selectivity for this enzyme relative to the numerous other serine hydrolases present in the human proteome in order to be therapeutically acceptable. Here we employed activity-based protein profiling (ABPP) to assess the selectivity of FAAH inhibitors in multiple rat and human tissues. We discovered that some inhibitors, including carbamate compounds SA-47 and SA-72, and AM404 are exceptionally selective while others, like URB597, BMS-1, OL-135, and LY2077855 are less selective, displaying multiple off-targets. Since proteins around 60 kDa constitute the major off-targets for URB597 and several other FAAH inhibitors with different chemical structures, we employed the multi-dimensional protein identification technology (MudPIT) approach to analyze their identities. We identified multiple carboxylesterase isozymes as bona fide off-targets of FAAH inhibitors. Consistently, enzymatic assay confirmed inhibition of carboxylesterase activities in rat liver by FAAH inhibitors. Since carboxylesterases hydrolyze a variety of ester-containing drugs and prodrugs, we speculate that certain FAAH inhibitors, by inhibiting carboxylesterases, might have drug–drug interactions with other medicines if developed as therapeutic agents.

© 2006 Elsevier Ltd. All rights reserved.

Keywords: FAAH; Inhibitor; ABPP; MudPIT; Carboxylesterase

1. Introduction

The endocannabinoid anandamide is a prototypical member of endogenous fatty acid amides that serves as signaling lipid messengers. It exerts neurobehavioral, cardiovascular, and immune-regulatory effects by activating cannabinoid (CB1

and CB2) and vanilloid (VR1) receptors (Di Marzo et al., 2002). Anandamide is synthesized in a stimulus-dependent manner and its signaling function is tightly controlled by the integral membrane enzyme fatty acid amide hydrolase (FAAH), which rapidly hydrolyzes anandamide and several other fatty acid amides to their corresponding acids (McKinney and Cravatt, 2005). Targeting the endocannabinergic system by inhibiting FAAH is a promising novel approach for the treatment of several nervous system disorders including pain, anxiety, and depression, as well as inflammation and hypertension (Cravatt and Lichtman, 2003). Mice lacking FAAH have significantly increased levels of certain fatty acid amides (Cravatt et al., 2001), including anandamide, and displayed analgesic (Cravatt et al.,

* Corresponding author. Neuroscience Research, Department R4PM, Building AP9-1125, Abbott Laboratories, 100 Abbott Park Road, Abbott Park, IL 60064-6118, USA. Tel.: +1 847 937 8271; fax: +1 847 937 9195.

E-mail address: di.zhang@abbott.com (D. Zhang).

¹ Present address: Proteomics Center, Stowers Institute for Medical Research, Kansas City, MO 64110, USA.

2001), anti-inflammatory (Massa et al., 2004) and increased responsiveness to anandamide-induced hypotension and cardio-depression (Pacher et al., 2005) phenotypes.

In addition to employing FAAH^{-/-} mice to evaluate the consequences of constitutive elevations in fatty acid amides, specific FAAH inhibitors would represent a valuable complementary approach and may have therapeutic utility for the treatment of a range of clinical disorders in both the central nervous system and periphery. This interest has led to the disclosure of a number of FAAH inhibitors, including the carbamates URB597 (Kathuria et al., 2003) and BMS-1 (Sit and Xie, 2002), α -keto-heterocycles OL-135 (Boger et al., 2005) and α -KH 7 (Leung et al., 2003), and α -keto oxadiazoles (Leung et al., 2005). Some anandamide re-uptake inhibitors, like AM404 (Beltramo et al., 1997; Glaser et al., 2003) and LY2077855 (Moore et al., 2005; Porter et al., 2004), also inhibit FAAH activity. Many of these FAAH inhibitors have recently been shown to produce beneficial behavioral effects in rodents. For example, URB597 produced CB1 receptor-dependent analgesia, anxiolytic, anti-depressive and anti-hypertensive effects (Batkai et al., 2004; Gobbi et al., 2005; Kathuria et al., 2003), CB2-dependent anti-inflammatory effects (Holt et al., 2005) and depressed alcohol-induced addiction (Perra et al., 2005). OL-135 and BMS-1 also had analgesic effects (Chang et al., 2006; Lichtman et al., 2004; Sit and Xie, 2002). AM404 produced antinociceptive (Beltramo et al., 1997) and hypotensive (Calignano et al., 1997) effects.

FAAH, a serine hydrolase, catalyzes the hydrolysis of its substrates using a highly conserved serine residue in its active site as the catalytic nucleophile. Many of the identified FAAH inhibitors, by possessing mechanism-dependent binding groups, exert their inhibitory effects by binding and modifying the catalytic serine residue, raising concerns that these agents may also inhibit other serine hydrolases. Therefore, evaluating the activity of FAAH inhibitors on other serine hydrolases is critical to define therapeutic potential of these agents.

However, determining the selectivity of FAAH inhibitors is a significant challenge, considering the immense size of the serine hydrolase superfamily, with more than 200 members in the human proteome. To address this problem, a proteomic strategy known as activity-based protein profiling (ABPP) was disclosed that permits the simultaneous assessment of all relevant competitive enzymes in a complex proteome (Leung et al., 2003). This approach involves preincubation of cell or tissue proteomes with FAAH inhibitors followed by addition of fluorophosphonate-based probes that were proved to react only with the catalytic serine in the enzymatic active site in an activity-dependent manner (Liu et al., 1999) and bear a reporter group (rhodamine, and biotin). The profile of proteins labeled by the reporter group is then visualized by gel electrophoresis. FAAH and off-target enzymes that are modified by inhibitors are incapable of reacting, or show reduced ability to react, with these probes, if they interfere with or compete for the same site, and this event can be detected by a reduction in signal intensity from the reporter group. The ABPP approach has been successfully employed to address the selectivity of several FAAH inhibitors (Leung et al., 2003; Lichtman et al., 2004).

More recently, multi-dimensional protein identification technologies (MudPITs) were employed to analyze the identities of potential target enzymes identified by the ABPP approach (Jessani et al., 2005). This combined ABPP–MudPIT technology allows a streamlined platform for high-content functional proteomic analysis.

In this report, we studied the selectivity of representative FAAH inhibitors to proteomes prepared from rat and human tissues. We identified multiple carboxylesterase isozymes as off-targets for URB597 and several other FAAH inhibitors. Considering that many carboxylesterases hydrolyze a variety of ester-containing drugs and prodrugs (Satoh and Hosokawa, 1998), we speculate that certain FAAH inhibitors might have drug–drug interactions if developed as therapeutic agents.

2. Material and methods

2.1. Chemicals

All chemicals were purchased from Aldrich Chemical Co. unless otherwise noted. Preparative RP-HPLC was performed on a Gilson Preparative system with a Waters radial compression Deltapak C18 column (25 × 200 mm) with a linear gradient of 5–80% acetonitrile in 0.1% TFA-water. Low-resolution mass spectra were obtained with a Finnigan SSQ7000 single quad mass spectrometer. Proton nuclear magnetic resonance (¹H NMR) spectra were recorded at 300 MHz (Varian Mercury 300). Chemical shifts are reported in ppm (δ) and coupling constants (J) are reported in hertz.

The fluorophosphonate-tetraethyleneglycol-tetramethyl rhodamine (FP-peg-TMR) and fluorophosphonate-tetraethyleneglycol-biotin (FP-peg-biotin) used as probes for ABPP were prepared by modifying the procedure described in the literature (Kidd et al., 2001; Patricelli et al., 2001). Briefly, *t*-butyl-dimethyl-silyl chloride was replaced with *t*-butyl-diphenyl-silyl chloride to improve the yield of reactions and to ease the monitoring of reaction status. The purification of intermediates was carried in less polar systems (dichloromethane–methanol system was replaced with dichloromethane–acetone system) to improve the quality of material. The full experimental procedure is provided as [Supplemental data](#).

URB597 (cyclohexyl-carbamic acid 3'-carbamoyl-biphenyl-3-yl ester), BMS-1 ([6-(2-methyl-4, 5-diphenyl-imidazol-1-yl)-hexyl]-carbamic acid 2-fluoro-phenyl ester), α -KH 7 ((*Z*)-1-(5-pyridin-2-yl-oxazol-2-yl)-octadec-9-en-1-one), SA-47 ([2-(6'-methyl-3,4,5,6-tetrahydro-2*H*-[1,2']bipyridinyl-4-yl)-ethyl]-carbamic acid methylcarbamoylmethyl ester), SA-72 ([3-[5-(6-methoxy-naphthalen-1-yl)-[1,3]dioxan-2-yl]-propyl]-carbamic acid carbamoylmethyl ester), and OL-135 (7-phenyl-1-(5-pyridin-2-yl-oxazol-2-yl)-heptan-1-one) were prepared essentially as described in the literature (Abouabdellah et al., 2005, 2006; Boger, 2004; Boger et al., 2005; Mor et al., 2004; Sit and Xie, 2002). AM404 (*N*-(4-hydroxyphenyl)-5*Z*,8*Z*,11*Z*,14*Z*-eicosatetrenamide) was purchased from Cayman Chemical, MI.

LY2077855 (5-(4-fluorobenzyl)-*N,N*-dimethyl-1*H*-tetrazole-1-carboxamide) was prepared according to the following procedure: 5-(4'-fluorobenzyl)-1,2,3,4-tetrazole (5.0 g, 28.0 mmol) was dissolved in dichloromethane (100 mL), followed by *N*-ethyl-*N,N*-diisopropylamine (7.7 mL, 44.2 mmol). The mixture was then cooled to 0 °C with an ice-water bath. Dimethylcarbamyl chloride (4.0 mL, 43.6 mmol) was added drop-wise. The reaction mixture was then allowed to warm up gradually overnight and quenched with K₂CO₃ (saturated). The organic layer was separated, and solvent removed under reduced pressure. The residue mixture was purified using HPLC (0.1% TFA) to give 820 mg (12%) desired product. ¹H NMR (CD₃OD, 300 MHz): δ = 7.32 ppm (m, 2H), 7.07 (m, 2H), 4.41 (s, 2H), 3.09 (s, 3H), 2.77 (s, 3H). MS (CI, M + 1): 250.0.

2.2. Cloning

To clone rat carboxylesterases X51974 (TGH, and ES10), NM_031565 (ES3), NM_133586 (ES2), NM_144743, NM_017004, X81825 (ES4), and

NM_001024365, the coding sequences were amplified by RT-PCR using poly A⁺ RNA from rat liver (Clontech, Palo Alto, CA) and cloned in pcDNA3.1/V5-His TOPO expression vector (Invitrogen, Carlsbad, CA). The gene-specific primers used in PCR amplifications are: X51974 (5'-ATGCGCCTCTA CCCTCTGGTC-3', 5'-GAGCTCAACATGTTCCAGTGG-3'), NM_031565 (5'-ATGTGCCTCTATGCTCTGATC-3', 5'-TAGCTCAGTGTGCTCCTGCAT G-3'), NM_133586 (5'-ATGGCACGGAACAACCACATAG-3', 5'-CAGCT CTGCATGGTTTTCTGAG-3'), NM_144743 (5'-ATGCCTTTGGCTAGAC TTCCTG-3', 5'-CAGCTCTGCATGCTTGCTCTG-3'), NM_017004 (5'-ATG TGGCTCTGTGTTCTGGTC-3', 5'-TGTGTGTTTCAGTGTGTTCTGTC-3'), X81825 (5'-ATGTGCCTCAGCTTCCTGATC-3', 5'-CAGCTCGTTGTGGTG TGGCTG-3'), and NM_001024365 (5'-ATGTGCCTCAGTCCCTGTT-3', 5'-CAGCTCATTGTGGTGGGGC-3').

2.3. Transfection and cell culture

Human embryonic kidney 293T (HEK293T) cells were cultured in Dulbecco's modified Eagle's medium (Invitrogen) supplemented with 10% fetal bovine serum (Invitrogen) and 1% penicillin–streptomycin (Invitrogen) in a humidified 5% CO₂, 95% O₂ incubator at 37 °C. Cells were transfected with the expression constructs using LipofectAMINE 2000 (Invitrogen) according to the manufacturer's instructions.

2.4. Whole cell proteome preparation

Rat and human tissues were purchased from Pel-Freez Biologicals Inc. (Rogers, AR) and Analytical Biological Services Inc. (Wilmington, DE), respectively. Tissues were homogenized using Tissue Tearor (Biospec Products, Bartlesville, OK) and cells were disrupted by sonication in a buffer containing 50 mM Tris pH 8.0, 320 mM sucrose, 10 μM E64, 20 μg/ml Bestatin, 1 μg/ml Pepstatin. After centrifugation at 5000g for 10 min, the supernatant yielded the whole cell proteomes.

2.5. Immunodepletion

To immunodeplete FAAH from cell or tissue extracts, 10 μg FAAH antibody (Cayman Chemical) was added to the extracts. After overnight incubation at 4 °C with gentle agitation, the immune complex was captured by Protein A agarose beads (Invitrogen) and removed by precipitation. Proteins in the extracts were resolved by SDS-PAGE (4–12% gel) and transferred to PVDF membrane for immunoblot analysis of the presence of FAAH.

2.6. Proteomic profiling of the selectivity of FAAH inhibitors

The activity-based proteomic profiling of inhibitor selectivity was essentially carried out as described previously (Leung et al., 2003). Briefly, proteome samples (1 mg/ml) were preincubated with inhibitors for 30 min and then mixed with 200 nM FP-peg-TMR at room temperature for 10 min. Reactions were quenched by the addition of SDS-PAGE loading buffer and heated at 70 °C for 10 min. Proteins were resolved by SDS-PAGE (4–12% gel) and visualized in-gel using a fluorescent scanner.

The intensities of protein bands were quantitated by ImageQuant (Amersham Biosciences, Piscataway, NJ). Samples treated with DMSO alone were considered 100% activity and band intensities that were diminished by inhibitors were expressed as a percentage of remaining activity. Data were collected from at least three trials at each inhibitor concentration and fit with a nonlinear regression curve using GraphPad Prism Software (GraphPad Software Inc., San Diego, CA). IC₅₀ values were calculated from the resulting dose–response curves.

2.7. Affinity purification of proteins labeled by FP-peg-biotin

The affinity purification of FP-peg-biotin labeled proteins from whole cell proteomes was carried out essentially as described previously (Kidd et al., 2001) with some modifications. Briefly, endogenous biotin-containing proteins from 1 to 3 mg tissue proteomes were precleared by incubating with 500 μl

neutravidin beads at 4 °C for 1 h. The proteomes were mixed with 4 μM FP-peg-biotin at room temperature for 20 min. Excess probes were cleared by passing the protein extracts over a Zeba desalt spin column (Pierce, Rockford, IL). Protein extracts eluted were treated with SDS (to 0.5% w/v), heated to 75 °C for 10 min, and then diluted threefold to bring down SDS concentration. The biotin labeled proteins were purified by incubating protein extracts with 100 μl streptavidin beads (Pierce) overnight, resolved by SDS-PAGE, and visualized by silver staining (Invitrogen). Protein bands of interest were excised from the gel for further analysis of protein identity.

2.8. MudPIT analysis of protein identities

The excised protein gel bands were digested and samples were then analyzed using nano-LC/MS/MS as previously described (Zhang et al., 2006). Each sample was loaded onto a 100 μm i.d. reverse-phase column aligned on-line with an ion-trap mass spectrometer. Peptides were eluted off the columns using an RP-gradient and sprayed directly into the inlet of mass spectrometer where they were subjected to fragmentation using CID. The resulting MS/MS spectra were interpreted using SEQUEST algorithm and data were generated using DTASelect/Contrast software. The filtered spectra were interpreted manually and only those proteins that were identified by good quality spectra were reported.

2.9. Carboxylesterase assay

Rat liver microsomes and cytosol, purchased from BD Biosciences (Woburn, MA), were used as sources of carboxylesterase to screen activity. Assays were conducted in 96-well microtiter plates at room temperature using a method described previously (Wheelock et al., 2001). Briefly, 0.5 μg liver microsomes or 2 μg cytosol were incubated with 10 μM FAAH inhibitor for 30 min and then substrate *p*-nitrophenyl acetate (Sigma) was added to a final concentration of 1 mM. The plate was read 10 min after substrate addition at 405 nm for the appearance of the *p*-nitrophenol using a Spectramax190 (Molecular Devices, Sunnyvale, CA). The carboxylesterase activities in liver extracts without inhibitor added were set at 100% and the remaining carboxylesterase activities after incubation with inhibitors were calculated relative to the control.

3. Results

3.1. Labeling FAAH by FP-peg-TMR

We synthesized FP-peg-TMR and assessed whether it can be used as a probe to detect FAAH and other serine hydrolases in an activity-dependent manner. Proteomes prepared from HEK293T cells and cells transfected with human FAAH were incubated with FP-peg-TMR probe and resolved by SDS-PAGE. Multiple fluorescent protein bands were observed that represent labeled serine hydrolases in the cells (Fig. 1). A strongly labeled 60 kDa protein band is present in FAAH transfected cells but not in untransfected HEK293T cells. This labeled protein band is missing when FAAH is immunodepleted by its antibody from FAAH transfected cells, indicating that this labeled 60 kDa protein is FAAH.

We also prepared proteomes from both rat and human brains and observed that multiple serine hydrolases were labeled by the FP-peg-TMR probe (Fig. 1). In rat brain, a single 60 kDa labeled band, which is missing when FAAH is immunodepleted from the proteome, represents FAAH. In human brain, a single 60 kDa labeled protein band was also observed; however, this labeled protein band remains largely unaffected when FAAH is immunodepleted from the proteome, indicating

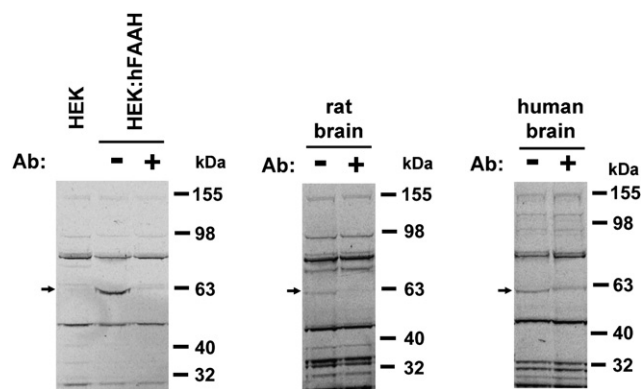


Fig. 1. Labeling FAAH by FP-peg-TMR. Serine hydrolases from proteomes prepared from cells or tissues as indicated are labeled by FP-peg-TMR. The 60 kDa FAAH band, indicated by an arrow, is present in HEK293T cells transfected with human FAAH (HEK:hFAAH), but not in untransfected HEK293T (HEK) cells. This labeled band is missing when FAAH is immunodepleted from FAAH transfected cells. In rat brain, the 60 kDa labeled protein band is FAAH that can be immunodepleted by antibody from the proteome. In human brain, the 60 kDa labeled protein band remains largely intact when FAAH is immunodepleted from the proteome.

that a serine hydrolase(s) other than human FAAH is the dominant protein labeled by the probe in this 60 kDa band.

3.2. Selectivity of URB597 and α -KH 7 in rat and human tissues

We addressed the selectivity of several representative FAAH inhibitors in proteomes prepared from rat and human tissues, and in the case of rat, we performed a comprehensive analysis by covering almost all major tissues. In addition, we assessed the selectivity in whole cell proteomes, rather than the membrane fraction as reported previously (Leung et al., 2003; Lichtman et al., 2004), in order to cover cytosolic as well as membrane-bound serine hydrolases.

Using proteomes prepared from HEK293T cells transfected with human FAAH, we first assessed the potency of the carbamate inhibitor URB597 (Kathuria et al., 2003) and the α -keto-heterocycle inhibitor α -KH 7 (Leung et al., 2003). As determined by the ABPP approach, URB597 inhibited FAAH with an IC_{50} of 0.109 μ M and α -KH 7 showed an IC_{50} of 0.077 μ M, which is comparable to the IC_{50} values determined by enzymatic assay (0.119 μ M for URB597 and 0.03 μ M for α -KH 7) by us (unpublished observations) and by others (Leung et al., 2003; Lichtman et al., 2004) using ABPP. We then prepared proteomes from 28 rat tissues and evaluated the selectivity of these two FAAH inhibitors at 10 μ M concentrations, which is about 100-fold over the IC_{50} values for URB597 and α -KH 7. Gel images from several representative tissues are shown in Fig. 2. In the neuronal tissues tested, including whole brain, cerebral cortex, cerebellum, hypothalamus and spinal cord, the labeling by FP-peg-TMR of only a single protein band around 60 kDa, which is FAAH, is competed off significantly by either URB597 or α -KH 7 while other protein bands remain visibly unaffected. In liver, heart, kidney, thyroid, prostate, bladder, lung, testicle, uterus,

lymph node, salivary gland, whole eye, epididymis, stomach, adrenal gland, pituitary and aorta, URB597 completely inhibits or diminishes the labeling of one or several protein bands around 60 kDa while not affecting the labeling of other bands on the gel. In intestine, in addition to the protein bands around 60 kDa, several protein bands around 50 and 40 kDa show diminished band intensity. However, no visible effects by URB597 on band patterns or intensities were observed in pancreas, thymus, muscle, spleen and ovary. As for α -KH 7, no visible changes in band intensity and pattern were observed in all 23 non-neuronal tissues tested, indicating exceptional selectivity for FAAH.

We next evaluated the selectivity of URB597 and α -KH 7 in four human tissues: brain, liver, heart and intestine (Fig. 3). URB597 competes the labeling of only one or two protein bands around 60 kDa in all four tissues, while other bands on the gel remain unaffected. α -KH 7 does not have any visible effects on labeled bands in any of the four human tissues.

3.3. Multiple FAAH inhibitors display broad specificity in rat and human tissues

We also evaluated the selectivity of other known FAAH inhibitors in whole cell proteomes prepared from representative rat and human tissues and the data are presented in Table 1. All inhibitors were assayed at a concentration of 10 μ M, in general representing approximately 100-fold or more above their IC_{50} values (our data or that reported in the literature), with the exception of AM404, which is a weaker inhibitor of FAAH. We assessed three other carbamate inhibitors besides URB597. BMS-1 (Sit and Xie, 2002) is much less specific for FAAH than URB597 in that it targeted several other labeled protein bands in addition to those around 60 kDa in all the rat and human tissues tested. SA-47 (Abouabdellah et al., 2006) and SA-72 (Abouabdellah et al., 2005) are also carbamate inhibitors, however, in contrast to URB597 and BMS-1, these two inhibitors showed exceptional selectivity for FAAH. OL-135 (Boger et al., 2005), an α -keto-heterocycle inhibitor similar to α -KH 7 is visibly not as specific as α -KH 7 in that it has a few off-targets mostly around 60 kDa in the tissues evaluated. We also assessed two anandamide re-uptake inhibitors, AM404 (Beltramo et al., 1997; Glaser et al., 2003) and LY2077855 (Porter et al., 2004), which have been reported to be FAAH inhibitors as well. AM404 also showed selectivity for FAAH. However, LY2077855 showed the poorest selectivity among all the inhibitors investigated in that it targeted many labeled protein bands in every tissue. This is consistent with a recent finding that a similar heterocyclic urea compound also showed poor selectivity (Alexander and Cravatt, 2006).

3.4. Identification of multiple carboxylesterases in the off-target bands around 60 kDa

Our selectivity screening revealed that proteins around 60 kDa constitute the off-targets for URB597 in rat and human

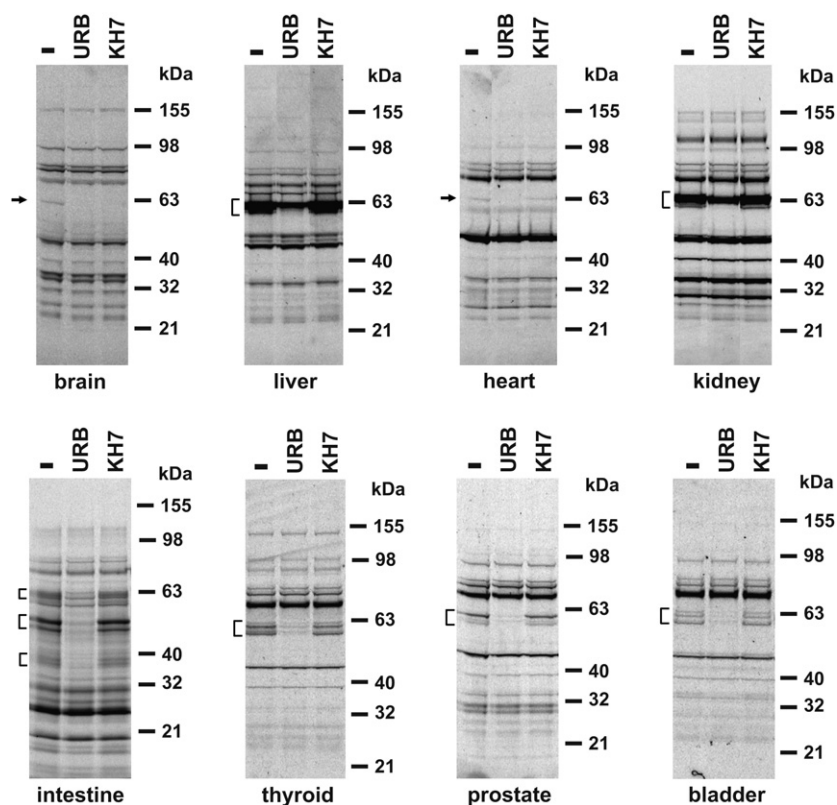


Fig. 2. Screening for the selectivity of URB597 and α -KH 7 in rat tissue proteomes. Competitive profiling reactions were set up in which 10 μ M FAAH inhibitor URB597 (URB) or α -KH 7 (KH7) competes with 200 nM FP-peg-TMR for the binding of serine hydrolases in rat tissue proteomes. Shown are fluorescent gel images of representative tissues as indicated and the missing or diminished protein bands are indicated by arrows or brackets, respectively.

tissues. These 60 kDa proteins are also frequent off-targets for other FAAH inhibitors evaluated. We then sought to isolate these potential off-targets by affinity purification and determine their identities by MudPIT analysis. To do this, an FP-peg-biotin probe was employed to label serine hydrolases in rat tissues and the labeled proteins were affinity-purified by streptavidin beads followed by separation on SDS-PAGE. Representative silver staining gels revealed similar patterns of protein bands labeled by FP-peg-biotin compared to those

labeled by FP-peg-TMR (Fig. 4). Protein bands around 60 kDa were excised from select tissues and were subjected to MudPIT analysis. The identities of multiple peptides were successfully revealed from liver, kidney and thyroid and were used to search Genbank for the corresponding genes (Table 2). We found that all the identified peptides correspond only to several carboxylesterase isozymes in rat with predicted molecular weight around 60 kDa. In liver, peptide(s) matching the sequences from carboxylesterases NM_017004, NM_133586

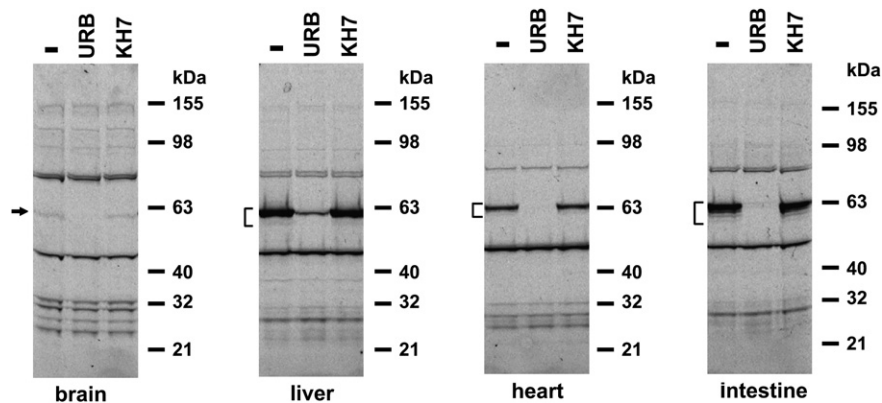
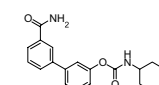
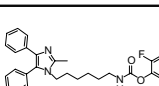
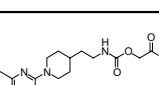
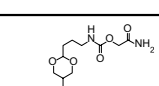
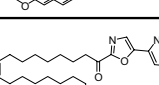
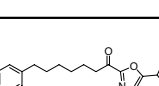
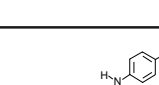
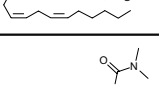


Fig. 3. Screening for the selectivity of URB597 and α -KH 7 in human tissue proteomes. Competitive profiling reactions were set up in which 10 μ M FAAH inhibitor URB597 (URB) or α -KH 7 (KH7) competes with 200 nM FP-peg-TMR for the binding of serine hydrolases in human tissue proteomes. Shown are fluorescent gel images and the missing or diminished protein bands are indicated by arrows or brackets, respectively.

Table 1
Selectivity profiling of FAAH inhibitors in representative rat and human tissues

Inhibitor	Structure	rat				human			
		Brain	Liver	Heart	Intestine	Brain	Liver	Heart	Intestine
URB597		1 (60)	2 (60)	1 (60)	1 (60), 2 (50), 3 (40)	1 (60)	2 (60)	1 (60)	2 (60)
BMS-1		1 (150), 1 (70), 1 (60)	2 (70), 2 (60), 2 (50), 1 (35)	1 (75), 1 (60), 1 (55), 1 (33)	1 (75), 1 (60), 2 (50), 2 (40), 1 (33)	1 (150), 1 (120), 1 (60), 2 (33)	1 (130), 1 (60), 3 (50–60), 1 (32)	1 (60), 1 (32)	1 (150), 2 (60), 1 (40)
SA-47		1 (60)							
SA-72		1 (60)							
α -KH 7		1 (60)							
OL-135		1 (60)	1 (60)	1 (60)	1 (60)	1 (60)	1 (130), 1 (60), 3 (50–60)	1 (60)	2 (60)
AM404		1 (60)							
LY2077855		11 (21–98)	14 (21–98)	8 (21–98)	20 (21–98)	2 (80), 1 (60), 3 (30–35)	10 (21–155)	1 (95), 1 (80), 1 (60), 2 (32), 1 (23)	2 (80), 2 (60), 1 (40), 3 (30)

The number of affected protein bands, if any, with the approximate range of molecular weight (in parentheses) is indicated for each inhibitor in a particular tissue proteome. The relative selectivity of FAAH inhibitors is categorized into four classes that are represented by different color schemes: exceptionally selective (green) with no visible change in band patterns except in rat brain the only protein band with diminished labeling is the 60 kDa FAAH band, highly selective (yellow) with only 1–2 visible missing or diminished protein bands, moderately selective (orange) with 3–5 visible affected protein bands, and poorly selective (red) with five or more affected protein bands.

(ES2), NM_144743, NM_001024365 and X81825 (ES4) were identified. A peptide matching several carboxylesterases including NM_017004 was identified in kidney. In thyroid, peptide(s) unique to NM_031565 (ES3) and NM_133586 (ES2) were identified.

3.5. FAAH inhibitors inhibit multiple carboxylesterases as off-targets

Considering that only a subset of the proteins identified in the 60 kDa range might actually be the off-targets of URB597, we proceeded to clone the matching carboxylesterases, expressed them in HEK293T cells, and evaluated which of these are indeed off-targets for URB597 (Fig. 5). URB597 strongly inhibits NM_001024365, NM_133586 (ES2) and NM_144743,

with IC₅₀ ranging from 0.21 μ M to 1.62 μ M. It weakly inhibits NM_031565 (ES3) with an IC₅₀ of 7.36 μ M. In contrast, URB597 does not inhibit NM_017004 at concentrations up to 100 μ M and is a very weak inhibitor for X81825 (ES4), with an IC₅₀ of 38.67 μ M.

We then evaluated whether these carboxylesterases are off-targets for other FAAH inhibitors (Fig. 6). We also included carboxylesterase X51974, which is rat TGH, in our analysis since TGH was shown to be an off-target for URB597 by others using mouse proteomes (Lichtman et al., 2004). Consistent with this, we found that, in addition to the carboxylesterases identified above (Fig. 5), URB597 also detectably inhibited rat TGH. All seven carboxylesterases are inhibited by BMS-1 and LY2077855 at 10 μ M concentration. In comparison, none of these carboxylesterases appeared to be off-targets for SA-47, SA-72, α -KH 7 or AM404. TGH, NM_133586 (ES2),

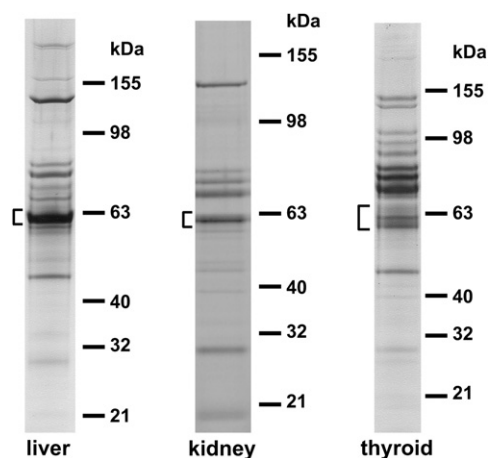


Fig. 4. Affinity purification of 60 kDa off-targets protein bands. Serine hydrolases in proteomes prepared from rat liver, kidney and thyroid were labeled with FP-peg-biotin and affinity-purified on streptavidin beads. Shown are silver-stained gels of purified proteins and protein bands of approximately 60 kDa (indicated by brackets) were excised for MudPIT analysis of protein identities.

X81825 (ES4) and NM_001024365 are inhibited by OL-135 at 10 μM concentration while NM_031565 (ES3), NM_144743 and NM_017004 are largely not affected. Overall, TGH was the most common off-target of the FAAH inhibitors assessed, closely followed by the carboxylesterases NM_001024365 and NM_133586 (ES2).

3.6. Inhibition of carboxylesterase activities in rat liver by FAAH inhibitors

Various carboxylesterases are present in a wide variety of organs and the highest activity occurs in the liver where multiple isozymes exist. Since FAAH inhibitors display broad inhibitory activities to carboxylesterases in our ABPP study, we set out to assess the effects of FAAH inhibitors on overall carboxylesterase activities in liver. Carboxylesterase activity of liver is found predominantly in the microsomal fraction. We thus incubated the microsomal fraction from rat liver with 10 μM FAAH inhibitors and then assayed for carboxylesterase

Table 2
Determination of off-target identities by MudPIT analysis of excised protein bands

Tissue	Representative peptide(s) identified	Corresponding gene cloned
Liver	A.PPEPAEPWSFVK.N	NM_017004
	R.GNWGYLDQVAALR.W	NM_133586 (ES2)
		NM_144743
	G.LKAEVAFWTQLLAK.R K.EEYLQIGATTQSQR.L K.YVSLEGVTQSVAVFLGVP FAKPPLGSLR.F	NM_001024365 X81825 (ES4)
Kidney	R.AISESGVVLTTNLDKK.N	NM_017004
Thyroid	K.AISESGVALTAGLVK.K	NM_031565 (ES3)
	K.SSFLNLPEEAIPVAEK.Y	
	K.LSGCEATDSETLVR.C	NM_133586 (ES2)

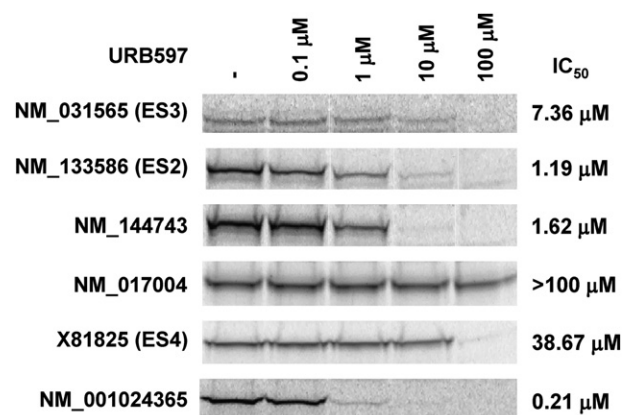


Fig. 5. Selectivity of URB597 against cloned carboxylesterases. Competitive profiling reactions were set up in which URB597 at the indicated dose competes with 200 nM FP-peg-TMR for the binding of carboxylesterases that were cloned and expressed in HEK293T cells. Shown are fluorescent gel images and the calculated IC_{50} values.

activities (Fig. 7A). Consistent with our ABPP study, SA-47 and SA-72, which are highly selective for FAAH, do not have major effects on the level of carboxylesterase activities in liver microsomes, while BMS-1 and LY2077855, the two inhibitors that target all seven cloned carboxylesterases, dramatically reduced the overall carboxylesterase activity levels in liver by about 90 and 95%, respectively. URB597 and OL-135, which display inhibitory effects on only a subset of carboxylesterases in our ABPP study, reduced the liver carboxylesterase activities to 50 and 70%, respectively. AM404, a weaker FAAH inhibitor, showed good selectivity at the concentration assayed. Although α -KH 7 does not have any visible effects on the seven cloned carboxylesterases in our ABPP study, we observed 20% reduction in carboxylesterase activity when added to the microsomal fraction of liver, suggesting that α -KH 7 may target other carboxylesterases which are yet to be identified. In addition to the microsomal fraction,

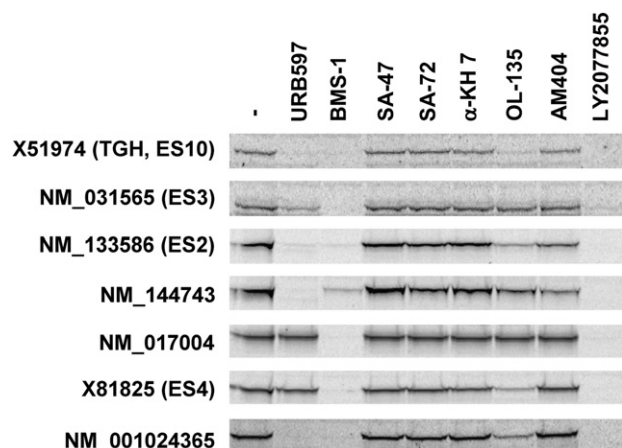


Fig. 6. Selectivity profiling of FAAH inhibitors against cloned carboxylesterases. Competitive profiling reactions were set up in which 10 μM FAAH inhibitors as indicated compete with 200 nM FP-peg-TMR for the binding of carboxylesterases that were cloned and expressed in HEK293T cells. Fluorescent gel images are shown.

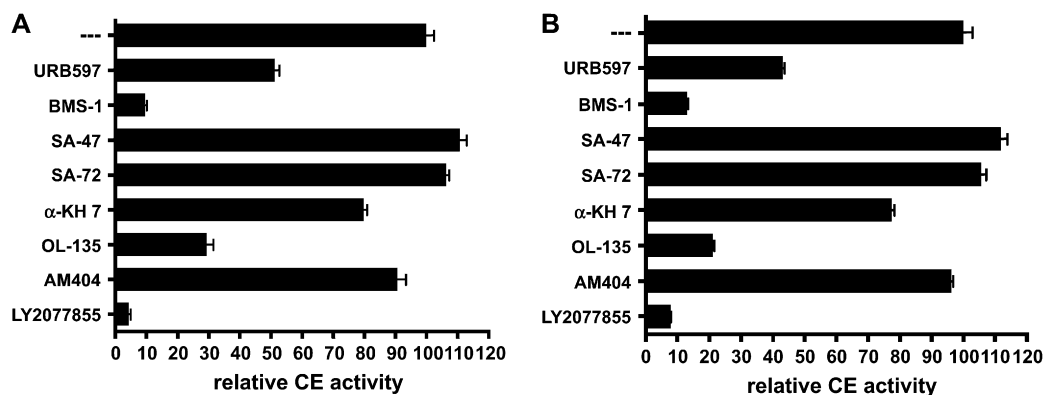


Fig. 7. Inhibition of liver carboxylesterase activities by FAAH inhibitors. Rat liver microsomes (A) or cytosol (B) were incubated for 30 min with 10 μ M FAAH inhibitors as indicated and then carboxylesterase (CE) activities were measured. Carboxylesterase activities relative to that without incubation with inhibitors are calculated and plotted as mean \pm SEM from five separate experiments of activity determination.

significant carboxylesterase activity is also present in the cytosol fraction of liver. The effects of FAAH inhibitors on the carboxylesterase activity levels in the cytosol were also evaluated and similar potencies of inhibition by these inhibitors were observed as those on the membrane-bound carboxylesterases in the microsome fraction (Fig. 7B).

4. Discussion

Activity-based probes have been increasingly employed in functional proteomics to profile enzyme activities globally in cells or tissues. In this report we employed the ABPP approach to study FAAH inhibitor selectivity among hundreds of serine hydrolases in the rat and human proteomes. We observed that FAAH inhibitors display broad specificity. SA-47 and SA-72 showed exceptional selectivity for FAAH. AM404 is also quite selective, although it is a relatively weaker inhibitor of FAAH. In addition, α -KH 7 appears selective in our ABPP study; however, it may target unidentified carboxylesterase(s) as revealed by enzyme assay. URB597, BMS-1, OL-135 and LY2077855 have off-target proteins across multiple rat and human tissues and their relative specificities are OL-135 > URB597 > BMS-1 > LY2077855. In some instances varied IC_{50} values for FAAH inhibitors have been reported in the literature, most likely due to differences in assay conditions. However, since we evaluated the selectivity of FAAH inhibitors at a concentration generally much higher than their IC_{50} values, the impact of such differences on interpretation of selectivity is reduced. Moreover, for some compounds such as URB597 and α -KH 7, we also generated IC_{50} values for FAAH within the ABPP assay. This therefore permitted a direct comparison, under the same assay conditions, between potency and selectivity for these compounds. To our knowledge, we are the first to report a comprehensive selectivity screening of FAAH inhibitors in rat and human and this study should provide valuable information for further development of these FAAH inhibitors or their analogs.

Due to the limited number of inhibitors evaluated, it is premature to correlate the specificity of an inhibitor to its chemical class or mechanism of inhibition. URB597,

BMS-1, SA-47 and SA-72 all have a carbamate group that may cause irreversible inactivation of FAAH through modification of its serine nucleophile. Interestingly, SA-47 and SA-72 are exceptionally specific while URB597 and BMS-1 have several off-targets. SA-47 and SA-72 are alkoxy carbamates whereas URB597 and BMS-1 are aryloxy carbamates. It is possible that, in part, the improved selectivity of SA-47 and SA-72 may derive from a reduction in inherent reactivity of the alkoxy moiety. However, other aspects of these molecules likely also contribute to their selectivity for FAAH. α -KH 7 and OL-135, both α -ketoheterocycles, inhibit FAAH reversibly (Boger et al., 2005; Leung et al., 2003) and both are relatively specific for FAAH, compared to the diversity in specificity of carbamate inhibitors. On the other hand, the heterocyclic urea compounds, LY2077855 (our study) and LY2183240 (Alexander and Cravatt, 2006), inhibit FAAH irreversibly and they are poorly selective. Selectivity may depend on orientation or accessibility of the inhibitor relative to key contact points within the active site as well as on amino acids involved in catalysis. In this respect, it is of interest that recent studies of the crystal structure of FAAH (Bracey et al., 2002), on molecular modeling with inhibitors (Mor et al., 2004), and on modeling of its catalytic mechanism (Lodola et al., 2005), suggest several unique features that may impact inhibitor selectivity. The active site of FAAH can potentially be accessed via membrane and cytosolic ports, with substrate bound at the active site and within an adjacent channel. Catalysis by FAAH has been proposed to occur via a novel mechanism, whereby lysine 142 accepts a proton from serine 217, which then deprotonates, and thereby creates the nucleophilic serine 241 of FAAH.

Although a unique pattern of labeled serine hydrolases was observed in each tissue in our study, some common serine hydrolases with apparent identical molecular weight and band intensity are often shared across multiple tissues. Notably, all neuronal tissues are very similar in their band patterns. We found that selective FAAH inhibitors remain selective across multiple tissues; however, less selective inhibitors often show common off-target bands across different tissues. For example, proteins around 60 kDa are major off-targets for

URB597 and are also frequent off-targets for other FAAH inhibitors in multiple tissues. Although we performed a comprehensive profiling of almost all major tissues in rat, it is possible to profile FAAH inhibitor specificity in a few representative tissues. Intestine, pancreas, stomach, liver and kidney are rich in diverse serine hydrolases and therefore can be employed in such screening.

Several off-targets for URB597, BMS-1 and OL-135 were identified previously in mouse proteomes, including TGH, AAD, CE-1, LPL, MAGL, KIAA1363 and CE6 (Alexander and Cravatt, 2005; Lichtman et al., 2004). We confirmed that carboxylesterases remain as off-targets in rat; although we found that rat TGH is an off-target for BMS-1 and OL-135 while the mouse counterpart was reported not to be an off-target (BMS-1) or only inhibited very weakly (OL-135). Also, in rats we did not observe effects on bands corresponding to the predicted molecular weight for the other reported off-targets. This discrepancy may be due to species differences in expression of off-targets or due to use of whole cell proteomes versus the more enriched membrane fraction used by Lichtman et al. (2004).

The most significant finding in this report is that we identified multiple carboxylesterase isozymes as novel off-targets for several structurally distinct FAAH inhibitors. These carboxylesterases were initially recovered from the 60 kDa protein band(s), which contain off-targets for URB597 and several other FAAH inhibitors. We then proved that they are bona fide off-targets using ABPP with cloned carboxylesterases. Further enzymatic assay confirmed the inhibitory effects of several FAAH inhibitors towards carboxylesterase activities in rat liver extracts.

Carboxylesterases (EC3.1.1.1) belong to the α/β hydrolase fold family with a nucleophile (serine), a base (histidine), and an acid (glutamic acid) forming the active site catalytic triad (Sato and Hosokawa, 1998). In contrast, FAAH contains a highly conserved amidase signature sequence and its catalytic mechanism appears to involve two serines and a lysine (Lodola et al., 2005; McKinney and Cravatt, 2005). Perhaps, although FAAH and carboxylesterases have very limited sequence homology, they share similar active site structures or features. In this respect, it is intriguing that the most common off-target we found is TGH, a carboxylesterase that can cleave triacylglycerol, thus sharing with FAAH the ability to cleave hydrophobic fatty acid-based molecules. In addition, these enzymes have complex active sites that accommodate a variety of substrates (Bracey et al., 2002; Dolinsky et al., 2004) and share the ability to cleave amide and ester bonds (Boger et al., 2000; Sato and Hosokawa, 1998).

Mammalian carboxylesterases represent a multigene family and at least eight rat isozymes have been identified (Furihata et al., 2005). More putative carboxylesterases, with sequence homology to the cloned enzymes, are reported in Genbank. Rat carboxylesterases are categorized into two families, CES1 and CES2, based on sequence homology (Sato and Hosokawa, 1998). However, we found no correlation between inhibition of these carboxylesterases and their sequence homology. For instance, X51974 (TGH, ES10), NM_031565 (ES3),

NM_017004, X81825 (ES4) and NM_001024365 are CES1 family members but respond differently to URB597 and OL-135. Moreover, although X81825 (ES4) and NM_001024365 share 93% sequence identity, NM_001024365 is significantly inhibited by URB597 whereas X81825 (ES4) is unaffected.

Carboxylesterases are present in a wide variety of tissues and the highest hydrolase activity occurs in the liver where multiple carboxylesterase isozymes exist (Sato and Hosokawa, 1998). We observed that select FAAH inhibitors inhibit carboxylesterase activities in both microsomal and cytosol fractions of liver. Although the relative expression levels of liver carboxylesterase isozymes is unknown due to the lack of specific antibodies, real time RT-PCR and Northern blot analyses nonetheless indicate dominant expression of X51974 (TGH, ES10), X81825 (ES4) and NM_031565 (ES3) in liver (Linke et al., 2005; Sanghani et al., 2002). Our ABPP study revealed potent inhibition of these three carboxylesterases by BMS-1 and LY2077855, and consistently only residual carboxylesterase activities remained when liver extracts were exposed to these inhibitors. Although the use of a general carboxylesterase substrate and liver extracts produced results that strongly support the ABPP data, this does not necessarily suggest that the enzymes identified by ABPP constitute the only carboxylesterases responsible for hydrolysis of the substrate. This notion is further supported by our observation that α -KH 7 inhibits carboxylesterase activities in liver by targeting unknown enzymes not identified in our ABPP study. Further studies with more specific substrates in enzymatic assays may help to assess the significance of in-tissue inhibition more precisely. Moreover, inhibition of an enzyme in vitro in the ABPP assay may not always translate to the in vivo situation. Although URB597 inhibits rat TGH in the ABPP study, it was recently reported that this compound does not significantly affect triolein hydrolysis in rat tissue that is rich in TGH (Clapper et al., 2006). Such a discrepancy might be dependent on the relative contribution of the enzyme to hydrolysis of a specific substrate in a tissue and/or may reflect potential differences in distribution, subcellular accessibility or metabolism of the inhibitor in the two different situations. Thus, although there appears to be a generally good correlation between effects in the ABPP assay and in tissue, caution should be taken in extrapolating data in this respect without subsequent assay.

A variety of compounds, such as organophosphates, trifluoromethyl ketone (TFK)-containing compounds and carbamates, block carboxylesterases as well as other esterases (Sato and Hosokawa, 1998). Potent and selective carboxylesterase inhibitors, such as benzil and sulfonamide classes of compounds, have also been identified (Wadkins et al., 2005, 2004). In this report, we confirmed that carbamate inhibitors URB597 and BMS-1, but not SA-47 or SA-72, inhibit carboxylesterases. In addition, we found that the α -ketoheterocycles, OL-135 and α -KH 7, inhibit carboxylesterases in our liver enzymatic study, albeit not as potently. Our ABPP study indicates that these two α -ketoheterocycle compounds, as well as URB597, are quite specific for carboxylesterases with few visible other targets except FAAH.

Carboxylesterases are broad-spectrum serine hydrolases that efficiently catalyze the hydrolysis of a variety of ester- and amide-containing chemicals to the respective free acids (Satoh and Hosokawa, 1998). They are involved in detoxification of structurally diverse xenobiotics, such as medicines, environmental chemicals, and endogenous substances with ester-, amide-, and thioester bonds. Carboxylesterases are also responsible for the metabolic activation of many prodrugs, such as the anti-tumor agent CPT-11 (Irinotecan), the chemotherapeutic drug capecitabine, and the blood cholesterol-lowering drug lovastatin (Liederer and Borchardt, 2006). Since a significant number of drugs or prodrugs are either eliminated or activated by these enzymes, altering carboxylesterase activity could have important clinical implications. For example, loperamide, which is administered concomitantly with capecitabine in cancer treatment, may diminish capecitabine effectiveness by inhibiting carboxylesterases required for its activation (Quinney et al., 2005). In this study, we found that several FAAH inhibitors can inhibit multiple carboxylesterases. This raises concern that some FAAH inhibitors, if advanced to the clinic, may affect the pharmacokinetic behavior of other therapeutic agents containing ester or amide bonds. Therefore, caution should be used if FAAH inhibitors and other drugs are co-administered, and the possible effects on drug elimination and prodrug activation should be carefully examined. In summary, the characterization of FAAH inhibitors using ABPP should aid in the identification of FAAH inhibitors of therapeutic value with reduced liability.

Appendix A. Supplementary information

Supplementary data associated with this article can be found, in the online version, at doi:10.1016/j.neuropharm.2006.11.009.

References

- Abouabdellah, A., Bas, M., Dargazanli, G., Hoornaert, C., Li, A.T., Medaiko, F., 2005. Derivatives of dioxane-2-alkyl carbamates, preparation thereof and application thereof in therapeutics. Patent US20050182130 A1.
- Abouabdellah, A., Burnier, P., Hoornaert, C., Jeunesse, J., Puech, F., 2006. Derivatives of piperidinyl- and piperazinyl-alkyl carbamates, preparation methods thereof and application of some in therapeutics. Patent US20060089344 A1.
- Alexander, J.P., Cravatt, B.F., 2005. Mechanism of carbamate inactivation of FAAH: implications for the design of covalent inhibitors and in vivo functional probes for enzymes. *Chem. Biol.* 12, 1179–1187.
- Alexander, J.P., Cravatt, B.F., 2006. The putative endocannabinoid transport blocker LY2183240 is a potent inhibitor of FAAH and several other brain serine hydrolases. *J. Am. Chem. Soc.* 128, 9699–9704.
- Batkai, S., Pacher, P., Osei-Hyiaman, D., Radaeva, S., Liu, J., Harvey-White, J., Offertaler, L., Mackie, K., Rudd, M.A., Bukoski, R.D., Kunos, G., 2004. Endocannabinoids acting at cannabinoid-1 receptors regulate cardiovascular function in hypertension. *Circulation* 110, 1996–2002.
- Beltramo, M., Stella, N., Calignano, A., Lin, S.Y., Makriyannis, A., Piomelli, D., 1997. Functional role of high-affinity anandamide transport, as revealed by selective inhibition. *Science* 277, 1094–1097.
- Boger, D.L., 2004. Inhibitors of fatty acid amide hydrolase. Patent WO2004033652 A2.
- Boger, D.L., Miyauchi, H., Du, W., Hardouin, C., Fecik, R.A., Cheng, H., Hwang, I., Hedrick, M.P., Leung, D., Acevedo, O., Guimaraes, C.R., Jorgensen, W.L., Cravatt, B.F., 2005. Discovery of a potent, selective, and efficacious class of reversible alpha-ketoheterocycle inhibitors of fatty acid amide hydrolase effective as analgesics. *J. Med. Chem.* 48, 1849–1856.
- Boger, D.L., Sato, H., Lerner, A.E., Hedrick, M.P., Fecik, R.A., Miyauchi, H., Wilkie, G.D., Austin, B.J., Patricelli, M.P., Cravatt, B.F., 2000. Exceptionally potent inhibitors of fatty acid amide hydrolase: the enzyme responsible for degradation of endogenous oleamide and anandamide. *Proc. Natl. Acad. Sci. U.S.A.* 97, 5044–5049.
- Bracey, M.H., Hanson, M.A., Masuda, K.R., Stevens, R.C., Cravatt, B.F., 2002. Structural adaptations in a membrane enzyme that terminates endocannabinoid signaling. *Science* 298, 1793–1796.
- Calignano, A., La Rana, G., Beltramo, M., Makriyannis, A., Piomelli, D., 1997. Potentiation of anandamide hypotension by the transport inhibitor, AM404. *Eur. J. Pharmacol.* 337, R1–R2.
- Chang, L., Luo, L., Palmer, J.A., Sutton, S., Wilson, S.J., Barbier, A.J., Breitenbucher, J.G., Chaplan, S.R., Webb, M., 2006. Inhibition of fatty acid amide hydrolase produces analgesia by multiple mechanisms. *Br. J. Pharmacol.* 148, 102–113.
- Clapper, J.R., Duranti, A., Tontini, A., Mor, M., Tarzia, G., Piomelli, D., 2006. The fatty-acid amide hydrolase inhibitor URB597 does not affect triacylglycerol hydrolysis in rat tissues. *Pharmacol. Res.* 54, 341–344.
- Cravatt, B.F., Demarest, K., Patricelli, M.P., Bracey, M.H., Giang, D.K., Martin, B.R., Lichtman, A.H., 2001. Supersensitivity to anandamide and enhanced endogenous cannabinoid signaling in mice lacking fatty acid amide hydrolase. *Proc. Natl. Acad. Sci. U.S.A.* 98, 9371–9376.
- Cravatt, B.F., Lichtman, A.H., 2003. Fatty acid amide hydrolase: an emerging therapeutic target in the endocannabinoid system. *Curr. Opin. Chem. Biol.* 7, 469–475.
- Di Marzo, V., De Petrocellis, L., Fezza, F., Ligresti, A., Bisogno, T., 2002. Anandamide receptors. *Prostaglandins Leukot. Essent. Fatty Acids* 66, 377–391.
- Dolinsky, V.W., Gilham, D., Alam, M., Vance, D.E., Lehner, R., 2004. Triacylglycerol hydrolase: role in intracellular lipid metabolism. *Cell. Mol. Life Sci.* 61, 1633–1651.
- Furuhata, T., Hosokawa, M., Fujii, A., Derbel, M., Satoh, T., Chiba, K., 2005. Dexamethasone-induced methylprednisolone hemisuccinate hydrolase: its identification as a member of the rat carboxylesterase 2 family and its unique existence in plasma. *Biochem. Pharmacol.* 69, 1287–1297.
- Glaser, S.T., Abumrad, N.A., Fatade, F., Kaczocha, M., Studholme, K.M., Deutsch, D.G., 2003. Evidence against the presence of an anandamide transporter. *Proc. Natl. Acad. Sci. U.S.A.* 100, 4269–4274.
- Gobbi, G., Bambico, F.R., Mangieri, R., Bortolato, M., Campolongo, P., Solinas, M., Cassano, T., Morgese, M.G., Debonnel, G., Duranti, A., Tontini, A., Tarzia, G., Mor, M., Trezza, V., Goldberg, S.R., Cuomo, V., Piomelli, D., 2005. Antidepressant-like activity and modulation of brain monoaminergic transmission by blockade of anandamide hydrolysis. *Proc. Natl. Acad. Sci. U.S.A.* 102, 18620–18625.
- Holt, S., Comelli, F., Costa, B., Fowler, C.J., 2005. Inhibitors of fatty acid amide hydrolase reduce carrageenan-induced hind paw inflammation in pentobarbital-treated mice: comparison with indomethacin and possible involvement of cannabinoid receptors. *Br. J. Pharmacol.* 146, 467–476.
- Jessani, N., Niessen, S., Wei, B.Q., Nicolau, M., Humphrey, M., Ji, Y., Han, W., Noh, D.Y., Yates 3rd, J.R., Jeffrey, S.S., Cravatt, B.F., 2005. A streamlined platform for high-content functional proteomics of primary human specimens. *Nat. Methods* 2, 691–697.
- Kathuria, S., Gaetani, S., Fegley, D., Valino, F., Duranti, A., Tontini, A., Mor, M., Tarzia, G., La Rana, G., Calignano, A., Giustino, A., Tattoli, M., Palmery, M., Cuomo, V., Piomelli, D., 2003. Modulation of anxiety through blockade of anandamide hydrolysis. *Nat. Med.* 9, 76–81.
- Kidd, D., Liu, Y., Cravatt, B.F., 2001. Profiling serine hydrolase activities in complex proteomes. *Biochemistry* 40, 4005–4015.
- Leung, D., Du, W., Hardouin, C., Cheng, H., Hwang, I., Cravatt, B.F., Boger, D.L., 2005. Discovery of an exceptionally potent and selective class

- of fatty acid amide hydrolase inhibitors enlisting proteome-wide selectivity screening: concurrent optimization of enzyme inhibitor potency and selectivity. *Bioorg. Med. Chem. Lett.* 15, 1423–1428.
- Leung, D., Hardouin, C., Boger, D.L., Cravatt, B.F., 2003. Discovering potent and selective reversible inhibitors of enzymes in complex proteomes. *Nat. Biotechnol.* 21, 687–691.
- Lichtman, A.H., Leung, D., Shelton, C.C., Saghatelian, A., Hardouin, C., Boger, D.L., Cravatt, B.F., 2004. Reversible inhibitors of fatty acid amide hydrolase that promote analgesia: evidence for an unprecedented combination of potency and selectivity. *J. Pharmacol. Exp. Ther.* 311, 441–448.
- Liederer, B.M., Borchardt, R.T., 2006. Enzymes involved in the bioconversion of ester-based prodrugs. *J. Pharm. Sci.* 95, 1177–1195.
- Linke, T., Dawson, H., Harrison, E.H., 2005. Isolation and characterization of a microsomal acid retinyl ester hydrolase. *J. Biol. Chem.* 280, 23287–23294.
- Liu, Y., Patricelli, M.P., Cravatt, B.F., 1999. Activity-based protein profiling: the serine hydrolases. *Proc. Natl. Acad. Sci. U.S.A.* 96, 14694–14699.
- Lodola, A., Mor, M., Hermann, J.C., Tarzia, G., Piomelli, D., Mulholland, A.J., 2005. QM/MM modelling of oleamide hydrolysis in fatty acid amide hydrolase (FAAH) reveals a new mechanism of nucleophile activation. *Chem. Commun. (Camb.)*, 4399–4401.
- Massa, F., Marsicano, G., Hermann, H., Cannich, A., Monory, K., Cravatt, B.F., Ferri, G.L., Sibaev, A., Storr, M., Lutz, B., 2004. The endogenous cannabinoid system protects against colonic inflammation. *J. Clin. Invest.* 113, 1202–1209.
- McKinney, M.K., Cravatt, B.F., 2005. Structure and function of fatty acid amide hydrolase. *Annu. Rev. Biochem.* 74, 411–432.
- Moore, S.A., Nomikos, G.G., Dickason-Chesterfield, A.K., Schober, D.A., Schaus, J.M., Ying, B.P., Xu, Y.C., Phebus, L., Simmons, R.M., Li, D., Iyengar, S., Felder, C.C., 2005. Identification of a high-affinity binding site involved in the transport of endocannabinoids. *Proc. Natl. Acad. Sci. U.S.A.* 102, 17852–17857.
- Mor, M., Rivara, S., Lodola, A., Plazzi, P.V., Tarzia, G., Duranti, A., Tontini, A., Piersanti, G., Kathuria, S., Piomelli, D., 2004. Cyclohexylcarbamate 3'- or 4'-substituted biphenyl-3-yl esters as fatty acid amide hydrolase inhibitors: synthesis, quantitative structure–activity relationships, and molecular modeling studies. *J. Med. Chem.* 47, 4998–5008.
- Pacher, P., Batkai, S., Osei-Hyiaman, D., Offertaler, L., Liu, J., Harvey-White, J., Brassai, A., Jarai, Z., Cravatt, B.F., Kunos, G., 2005. Hemodynamic profile, responsiveness to anandamide, and baroreflex sensitivity of mice lacking fatty acid amide hydrolase. *Am. J. Physiol. Heart Circ. Physiol.* 289, H533–H541.
- Patricelli, M.P., Giang, D.K., Stamp, L.M., Burbaum, J.J., 2001. Direct visualization of serine hydrolase activities in complex proteomes using fluorescent active site-directed probes. *Proteomics* 1, 1067–1071.
- Perra, S., Pillolla, G., Melis, M., Muntoni, A.L., Gessa, G.L., Pistis, M., 2005. Involvement of the endogenous cannabinoid system in the effects of alcohol in the mesolimbic reward circuit: electrophysiological evidence in vivo. *Psychopharmacology (Berl.)*, 1–10.
- Porter, A.C., Li, J., Love, P.L., Shannon, H.E., Li, D.L., Phebus, L.A., Gleason, S.D., Witkin, J.M., Simmons, R.M.A., Iyengar, S., Nomikos, G.G., 2004. LY2077855: a novel, potent, selective, non-endocannabinoid related inhibitor of anandamide inactivation demonstrates robust analgesic effects in an in vivo pain model. *Soc. Neurosci. (Program No. 273.11)*.
- Quinney, S.K., Sanghani, S.P., Davis, W.I., Hurley, T.D., Sun, Z., Murry, D.J., Bosron, W.F., 2005. Hydrolysis of capecitabine to 5'-deoxy-5-fluorocytidine by human carboxylesterases and inhibition by loperamide. *J. Pharmacol. Exp. Ther.* 313, 1011–1016.
- Sanghani, S.P., Davis, W.I., Dumauval, N.G., Mahrenholz, A., Bosron, W.F., 2002. Identification of microsomal rat liver carboxylesterases and their activity with retinyl palmitate. *Eur. J. Biochem.* 269, 4387–4398.
- Satoh, T., Hosokawa, M., 1998. The mammalian carboxylesterases: from molecules to functions. *Annu. Rev. Pharmacol. Toxicol.* 38, 257–288.
- Sit, S.Y., Xie, K., 2002. Bisarylimidazolyl fatty acid amide hydrolase inhibitors. Patent US 6562846 B2.
- Wadkins, R.M., Hyatt, J.L., Wei, X., Yoon, K.J., Wierdl, M., Edwards, C.C., Morton, C.L., Obenauer, J.C., Damodaran, K., Beroza, P., Danks, M.K., Potter, P.M., 2005. Identification and characterization of novel benzil (diphenylethane-1,2-dione) analogues as inhibitors of mammalian carboxylesterases. *J. Med. Chem.* 48, 2906–2915.
- Wadkins, R.M., Hyatt, J.L., Yoon, K.J., Morton, C.L., Lee, R.E., Damodaran, K., Beroza, P., Danks, M.K., Potter, P.M., 2004. Discovery of novel selective inhibitors of human intestinal carboxylesterase for the amelioration of irinotecan-induced diarrhea: synthesis, quantitative structure–activity relationship analysis, and biological activity. *Mol. Pharmacol.* 65, 1336–1343.
- Wheelock, C.E., Severson, T.F., Hammock, B.D., 2001. Synthesis of new carboxylesterase inhibitors and evaluation of potency and water solubility. *Chem. Res. Toxicol.* 14, 1563–1572.
- Zhang, D., Chen, J., Saraf, A., Cassar, S., Han, P., Rogers, J.C., Brioni, J.D., Sullivan, J.P., Gopalakrishnan, M., 2006. Association of *catsper1* or *-2* with *Cav3.3* leads to suppression of T-type calcium channel activity. *J. Biol. Chem.* 281, 22332–22341.